(Preprint) AAS 17-731

ORBIT DESIGN FOR A PHOBOS-DEIMOS CYCLER MISSION

Bolys Sabitbek[*], Brian C. Gunter[†]

Little is know about the Martian moons Phobos and Deimos, even though they have the potential to provide insight into the evolution of the Martian system, and could potentially serve as a staging site for a future Mars manned mission. While attempts to visit Phobos with dedicated missions have been attempted, to date none have been successful, and no dedicated mission to Deimos has been flown. As such, much of what is known about the structure and composition of either moon comes from a small collection of images. This study explores a class of stable cycler orbits that could visit both moons on a regular cadence, and can be tuned to fly-by one moon more frequently, or to vary the ground track coverage to obtain improved surface coverage. While the orbits described can be reached by a dedicated spacecraft with sufficient delta-V for a Mars insertion, the motivation here is that the spacecraft is already in an initial insertion orbit, such as a small-satellite rideshare on an existing Mars mission. Under this assumption, the results presented illustrate that the exploration of both Phobos and Deimos can be achieved with a spacecraft with capabilities of modern nanosatellites (cubesats).

INTRODUCTION

The first missions to provide the images of Phobos and Deimos were part of the U.S. Mariner (1969) and Viking (1977) satellite programs, as well as the Soviet Phobos Program (1988). The three dedicated missions designed by the former U.S.S.R and Russian Federation (Phobos 1, Phobos 2, and Phobos-Grunt), which were to approach the Phobos at close range (50 m) and then land on the surface,[1,2] each experienced various technical problems that resulted in early mission failures. While later Mars missions, such as Mars Express (ESA) and the Mars Reconnaissance Orbiter (US) would gather additional imaging and spectrometer data,[3,4] the total number of images and their spectral and spatial resolution is still quite limited. As a result, very little is still known about the composition and evolution of either Phobos or Deimos.

Interest in the Mars system is still strong, with a number of robotic and potential manned missions planned for the future. To date, only the Japanese-led Martian Moons eXploration (MMX)* mission is slated to visit Phobos or Deimos, with an anticipated launch in late 2024. Other missions are scheduled for Mars before then, which could easily accommodate a small rideshare satellite that could be deployed as a secondary mission to gather valuable imagery and potential field data with low cost and risk. It is this notion that has motivated the current study into various orbits within the Mars system that would allow both moons to be explored with minimal resources.

A number of prior studies have explored such rendezvous orbits within the Mars system, starting with early efforts by Taylor and Faust,[5] and Tolson et al,[6] involving the Viking missions. Gill and

[*]Graduate Student, Daniel Guggenheim School of Aerospace Engineering, North Ave NW, Atlanta, GA 30332
[†]Assistant Professor, Daniel Guggenheim School of Aerospace Engineering, North Ave NW, Atlanta, GA, 30332 Senior Member AIAA
*http://mmx.isas.jaxa.jp/en/

Schwarz (2010)[7] analyzed Quasi-Satellite Orbits (QSOs) around Phobos. Quasi-satellite orbits are a special type of orbit in the three body problem where one of the primaries has a much larger mass than the other, i.e., $m_1 \gg m_2$. QSOs are not closed periodic trajectories, although they tend to occupy the same region in space. QSOs are also known as distant retrograde orbits, DROs, or instant satellite orbits, and is the orbit strategy likely to be implemented for the MMX mission. In addition to QSOs, Wallace et al[8] discussed other options available for missions around Phobos and Deimos, such as fixed-point station keeping or hovering orbits and Lagrange-point orbits. Additional studies include the work of Zamora and Biggs,[9] who extended the model of the circular restricted three body problem (CR3BP) to consider the orbital eccentricity and the highly-inhomogeneous gravity field of Phobos, by incorporating the gravity harmonics series expansion into an elliptic R3BP, named ER3BP-GH. Following this, the dynamical substitutes of the Libration Point Orbits (LPOs) are computed in this more realistic model of the relative dynamics around Phobos, combining methodologies from dynamical systems theory and numerical continuation techniques. Results obtained show that the structure of the periodic and quasi-periodic LPOs differs substantially from the classical case without harmonics. Several potential applications of these natural orbits are presented to enable unique low-cost operations in the proximity of Phobos, such as close- range observation, communication, and passive radiation shielding for human spaceflight.

Most of these earlier studies focus almost exclusively on Phobos, or treat Phobos and Deimos as separate cases for which dedicated QSO or LROs can be developed. To maximize the scientific return of a single satellite, this study seeks a class of orbits that would potentially visit both moons regularly, such as a cycler mission. Genova et al[10] recently proposed a particular Phobos-Deimos cycler orbit for a specific mission concept proposal, which was inspired by the earlier Viking rendezvous orbits. This study explores the Phobos-Deimos cycler orbit in a more generic sense, examining a wide range of potential options, and their subsequent revisit times and required ΔVs. It is assumed that the primary scientific objective for the Phobos-Deimos cycler mission is to obtain high-resolution imagery, meaning the spacecraft was targeted to encounter between 50 km and 150 km on different sides of Phobos and Deimos. While the orbits described here can be reached by a dedicated spacecraft, the intention here is that the spacecraft is already in an initial insertion orbit, such as a small-satellite rideshare on an existing Mars mission. Under this assumption, the results presented illustrate that the exploration of both Phobos and Deimos is possible with a spacecraft with capabilities of modern nanosatellites (cubesats).

METHODOLOGY

Resonance Analysis

The orbital periods of Phobos and Deimos are 7.64 and 30.312 hours, respectively, putting the two moons in a natural 4:1 resonance. This resonance permits the determination of all possible orbits that would have mean-motion resonance to both Phobos and Deimos. These Double Resonant Orbits (DROs) are the orbits that have mean-motion resonance with Phobos and Deimos under the conditions where the pericenter of the DROs is equal to the semi-major axis of Phobos and the apocenter of the DROs is equal to or greater than the semi-major axis of Deimos. If the orbiting periods of the DROs have some ratio with Phobos or Deimos, the mean motions n would satisfy the following

$$k_1 n - k_2 n_{p/d} = 0 \tag{1}$$

where

$$n_{p/d} = \frac{2\pi}{T_{p/d}} \tag{2}$$

and $T_{p/d}$ is the orbital period of Phobos or Deimos, with k_1 and k_2 being rational numbers. Then, using n we can find the orbit elements with the following

$$T = \frac{2\pi}{n}, \tag{3}$$

$$a = \left(\frac{T\sqrt{(\mu)}}{2\pi} \right)^{2/3}, \tag{4}$$

$$e = \frac{2(a - r_p)}{2a}, \tag{5}$$

where r_p is the distance of periapasis.

Orbit Trajectories

Figure 1 shows a representative encounter geometry at the instant of the orbit intersection between Phobos, Deimos and a DRO in a view from near the Martian North Pole (i.e., with the Mars center of mass located at the plot origin). The nearly circular orbit of Phobos and Deimos have a radius of approximately 9376 km and 23463.2 km with an inclination of about 1 deg. The periapsis altitude of the DRO shown was approximately 9234 km. Fig. 1 shows that an orbit intersection between Phobos and DROs occurs along the periapsis of DROs. The intersection between Deimos and DROs occurs along the line of nodes at the descending crossing.

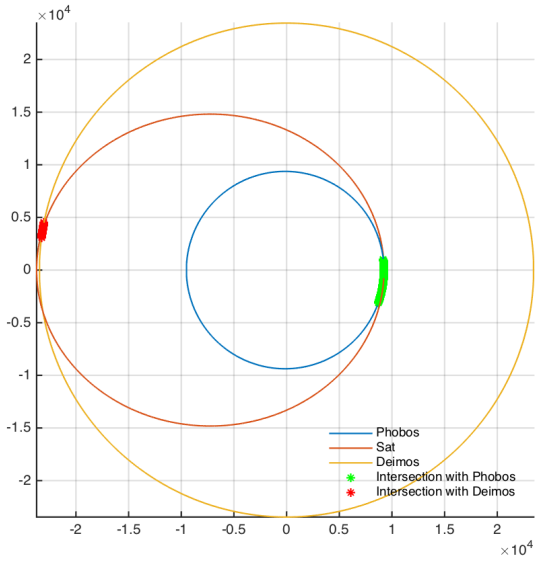

Figure 1: Encounter geometry of the Phobos, Deimos and Double-Resonance Orbits.

The well known conic equation

$$r = \frac{a(1 - e^2)}{1 + e\cos f} \tag{6}$$

is also used, where r is the spacecraft distance from Mars, a is the semi-major axis, e is the eccentricity and f is the true anomaly. The true anomaly f can be used to calculate the approximate value of the argument of periapsis, ω, required for orbit intersection. Since both moons have an inclination near zero, the spacecraft will intercept them when $f \approx \omega$ (ascending node) and when $f \approx 180 - \omega$ (descending node). Assuming each moon is in an exactly circular orbit, there will be an intersection with the DROs when r equals the semi-major axis of Phobos or Deimos orbit.

Perturbations on the spacecraft's orbit change this initial orbit geometry. The major perturbation, the oblateness of Mars, produces both a nodal regression and an apsidal precession, given by

$$\dot{\Omega} = -n\frac{3}{2}J_2 \cos i \left(\frac{R}{a}\right)^2 \frac{1}{(1-e^2)^2}, \tag{7}$$

$$\dot{\omega} = n\frac{3}{2}J_2 \left(\frac{R}{a}\right)^2 \left(2 - \frac{5}{2}\sin^2 i\right) \frac{1}{(1-e^2)^2}, \tag{8}$$

where J_2 is $1.96 \cdot 10^{-3}$, n is the mean-motion of spacecraft orbit, R =3394 km is the radius of Mars used as reference for gravity field expansion, a is the semi-major axis of the spacecraft orbit, i is the inclination. The orbital parameters h,a,e and i do not change substantially with time.

ΔV analysis

Once we have $\Delta\omega$ from equation (8), we must find the Δv_1 value to achieve the desired correction. The amount of Δv_1 required depends on the magnitude of the correction $|\Delta\omega|$, the direction of the thrust vector in the orbital plane, and the location in the orbit where the burn is executed.

$$\Delta\omega = \frac{\sqrt{1-e^2}}{nae}\left(1 + \frac{r}{p}\right)\sin f \Delta v_1 \tag{9}$$

We can show that the most efficient burn is in the transverse direction at $f = \pm 90°$. Thus,

$$\Delta\omega = \frac{2\sqrt{1-e^2}}{nae}\Delta v_1 \tag{10}$$

and the Δv_1 magnitude is

$$\Delta v_1 = \frac{nae}{2\sqrt{1-e^2}}\,|\Delta\omega| \tag{11}$$

RESULTS

Using the methodology described above, a resonance analysis was conducted for the Phobos and Deimos orbits, with the results summarized in Fig. 2 and Tbl. 1. As seen in Fig. 2, at least fourteen resonant spacecraft orbits intersect both moons on a regular cadence. The notation for the resonances represent the number of orbits of the moon that coincide with the number of orbits of the spacecraft. For example, the 8:3 resonance for Phobos means that Phobos will make 8 orbits about Mars and the spacecraft will make 3 orbits before the two will meet again, and that there will also be at least one encounter with Deimos during this cycle. Tbl. 1 also provides information on the ΔV requirements to maintain the given cycler orbit given the dominant J2 perturbation from Mars (column ΔV_1), as well as the ΔV required to achieve the initial orbit from an initial starting orbit similar to that of the Mars Reconnaissance Orbiter (column ΔV_2), which is at an altitude of approximately 300km.

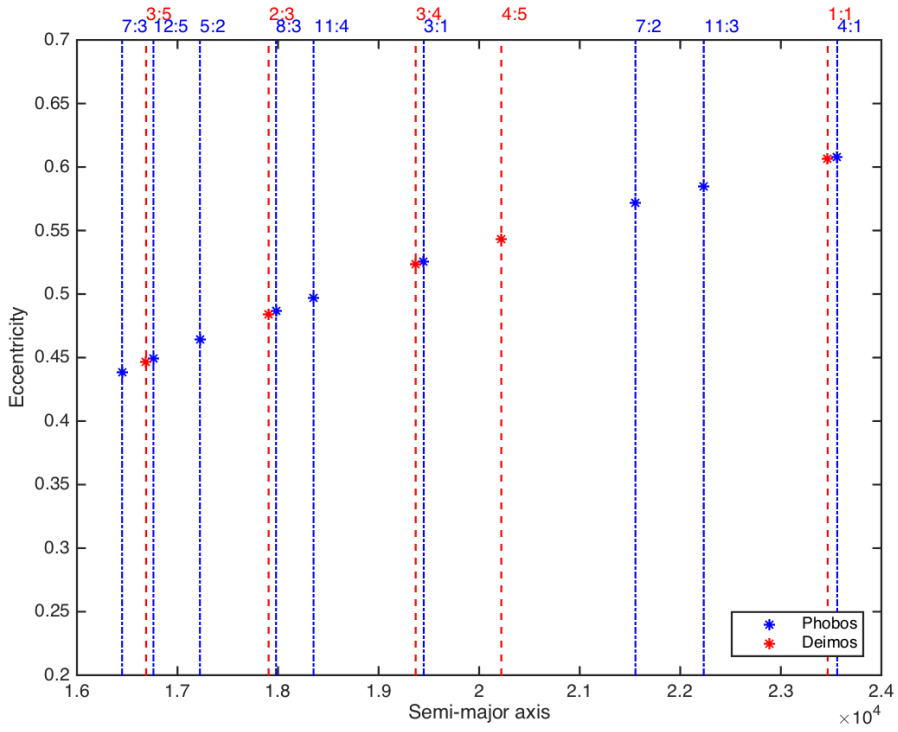

Figure 2: Summary of Phobos and Deimos orbit resonances

Table 1: Orbit characteristics of candidate resonant orbits

N	R	a (km)	T (day)	e	r_a (km)	ω_d (deg)	$\dot{\Omega}$ (deg/day)	$\dot{\omega}$ (deg/day)	ΔV_1 (m/s)	ΔV_2 (km/s)
Phobos										
1	7:3	16490.3	0.7441	0.4393	23734.4	170.00	-0.0925	0.1850	0.4734	1.4021
2	12:5	16802.9	0.7654	0.4497	24359.7	163.03	-0.0887	0.1773	0.4760	1.3890
3	5:2	17266.5	0.7973	0.4645	25286.8	155.98	-0.0840	0.1680	0.4808	1.3702
4	8:3	18025.6	0.8472	0.4871	26805.0	148.51	-0.0764	0.1528	0.4852	1.3410
5	11:4	18399.2	0.8737	0.4975	27552.2	145.75	-0.0730	0.1461	0.4870	1.3274
6	3:1	19498.1	0.9552	0.5258	29749.9	139.53	-0.0645	0.1290	0.4912	1.2894
7	7:2	21554.2	1.1119	0.5716	33874.3	131.84	-0.0521	0.1040	0.4960	
8	11:3	22289.1	1.1649	0.5852	35331.9	130.04	-0.0489	0.0978	0.4970	1.2060
9	4:1	23620.2	1.2708	0.6086	37994.3	127.11	-0.0435	0.0870	0.4983	1.1715
Deimos										
10	3:5	16691.7	0.7576	0.4461	24137.3	164.52	-0.0902	0.1804	0.4768	1.3936
11	2:3	17906.3	0.8420	0.4836	26566.5	149.12	-0.0771	0.1542	0.4848	1.3455
12	3:4	19369.1	0.9472	0.5226	29491.9	139.90	-0.0651	0.1301	0.4910	1.2937
13	4:5	20220.6	1.0104	0.5427	31195.0	136.24	-0.0594	0.1188	0.4934	1.2662
14	1:1	23463.9	1.2632	0.6059	37681.7	127.30	-0.0439	0.0877	0.4982	1.1754

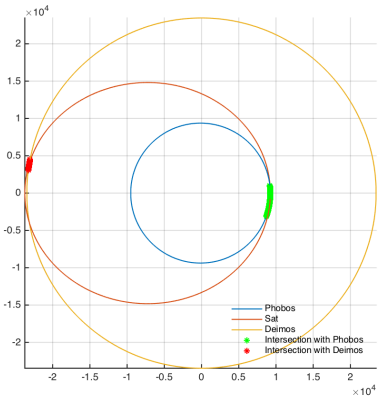

(a) Orbit trajectories

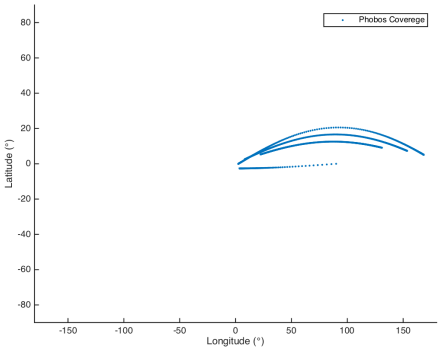

(b) Phobos Ground Track

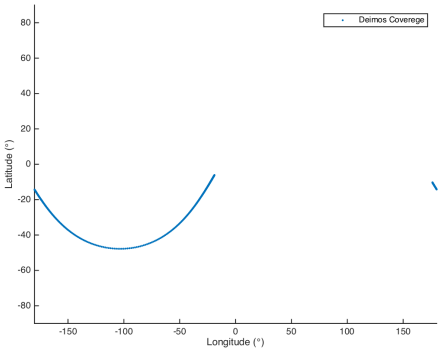

(c) Deimos Ground Track

Figure 3: a) Resonance orbit 7:3, with corresponding ground tracks for b) Phobos and c) Deimos

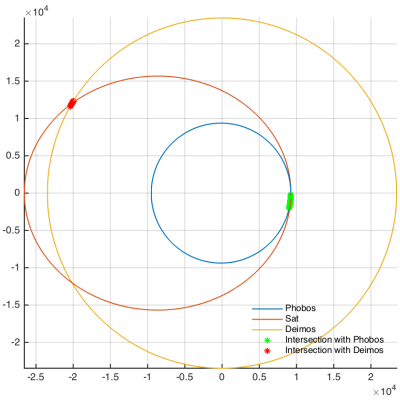

(a) Orbit trajectories

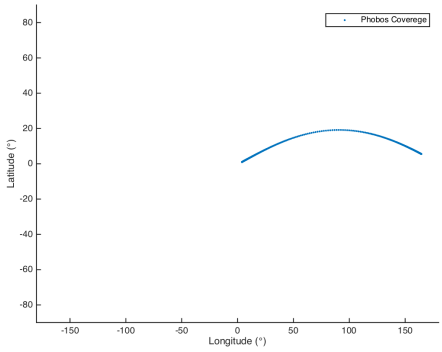

(b) Phobos Ground Track

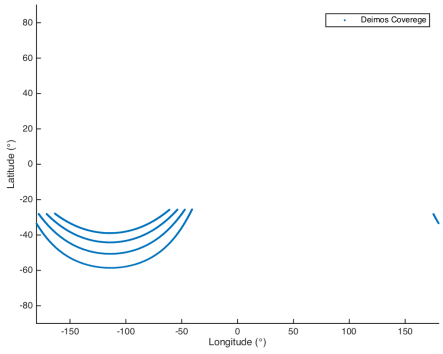

(c) Deimos Ground Track

Figure 4: a) Resonance orbit 2:3, with corresponding ground tracks for b) Phobos and c) Deimos

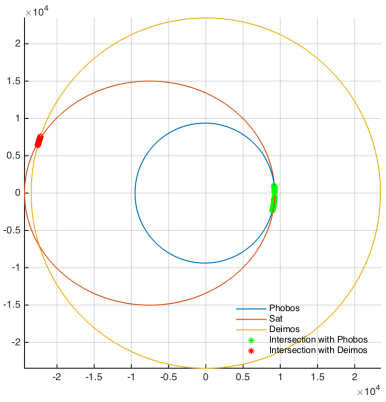

(a) Orbit trajectories

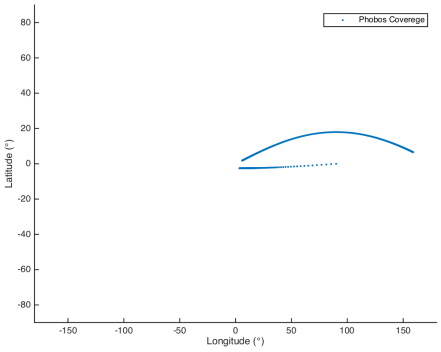

(b) Phobos Ground Track

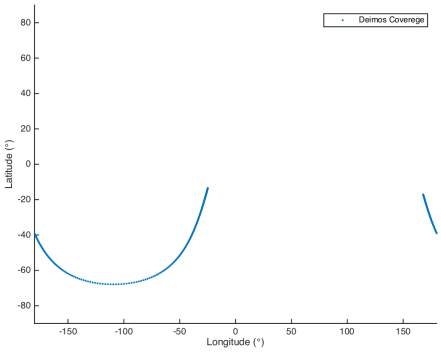

(c) Deimos Ground Track

Figure 5: a) Resonance orbit 12:5, with corresponding ground tracks for b) Phobos and c) Deimos

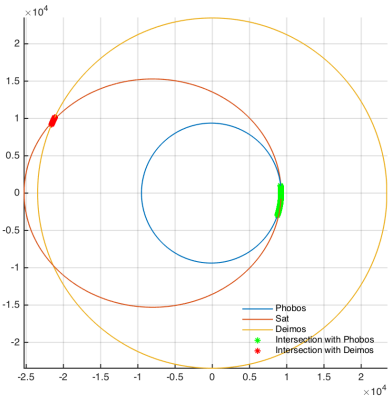

(a) Orbit trajectories

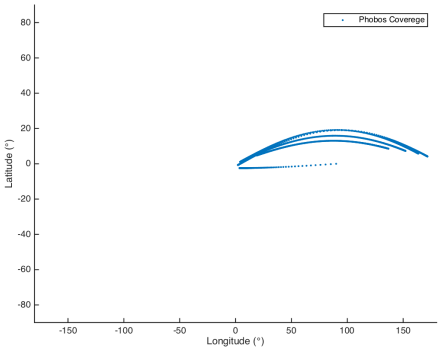

(b) Phobos Ground Track

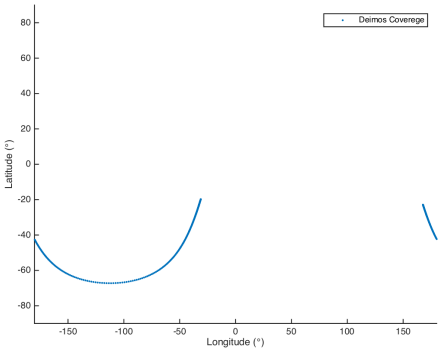

(c) Deimos Ground Track

Figure 6: a) Resonance orbit 5:2, with corresponding ground tracks for b) Phobos and c) Deimos

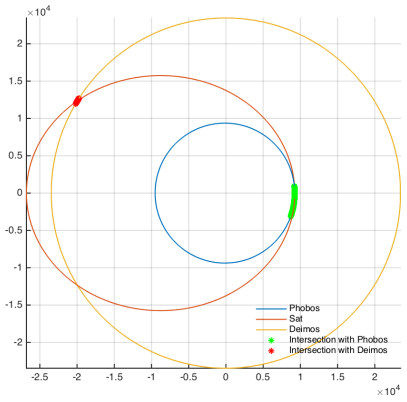

(a) Orbit trajectories

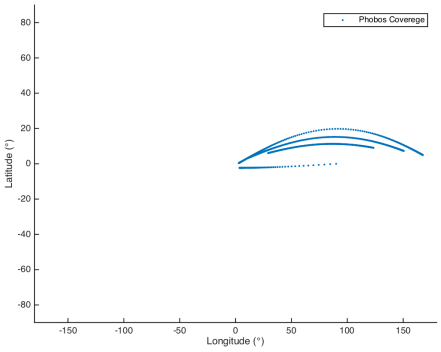

(b) Phobos Ground Track

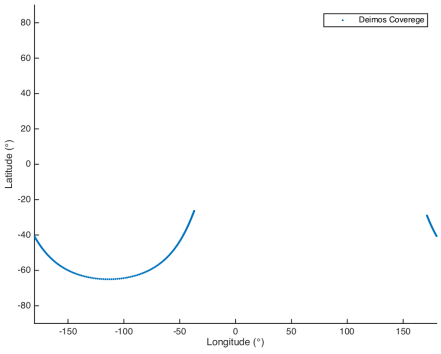

(c) Deimos Ground Track

Figure 7: a) Resonance orbit 8:3, with corresponding ground tracks for b) Phobos and c) Deimos

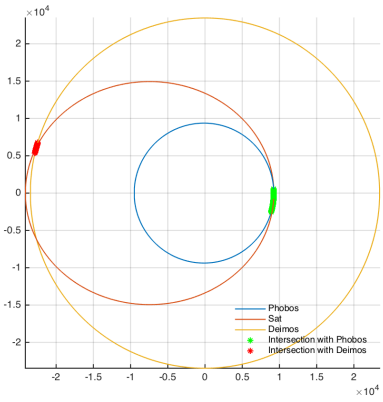

(a) Orbit trajectories

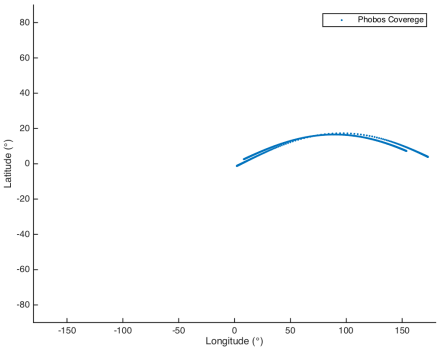

(b) Phobos Ground Track

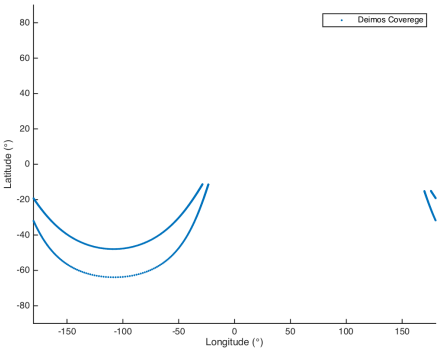

(c) Deimos Ground Track

Figure 8: a) Resonance orbit 3:5, with corresponding ground tracks for b) Phobos and c) Deimos

In addition to the numerical data, Figs. 3-8 provide additional visualizations of six cycler candidates in terms of orbit geometry and ground track coverage on both Phobos and Deimos over the span of one (Earth) week. For the geographical plots of the ground tracks, an orbit inclination of 0.5 degrees is used. The behavior and relative stability of all cycler orbits were also verified through extensive testing using NASA's General Mission Analysis Tool (GMAT)*. Though not shown here, it is important to note that the location of the ground track passes can be changed using small maneuvers as part of the station keeping. This means that much greater coverage can be achieved with subsequent cycles, or targeted repeat measurements can be made. In addition, the ΔV requirements to transition between different cycler orbit resonances is not prohibitive either, meaning that the spacecraft could operate in various cycler orbit throughout the mission to satisfy different mission objectives, e.g., if more frequent observations of Deimos were desired over a specific phase of the mission.

CONCLUSION

In this work, a class of resonant cycler orbits was explored with intent of visiting both Phobos and Deimos for gathering remote sensing observations. A resonance analysis identified 14 distinct cycler orbits that intersect Phobos and Deimos at least once per cycle. The orbits are relatively stable, requiring only modest ΔV requirements (¡ 0.5 m/s per week) for maintenance maneuvers. Furthermore, to reach the cycler orbit from an initial MRO-style orbit requires on the order of 1.5 km/s of ΔV. This is now within, or close to, the realm of propulsion capabilities for small satellites, with commercial electrospray and Hall-effect vendors now advertising 1-2 km/s performance for a 6U sized spacecraft (where 1U = 10 x 10 x 10 cm in volume and 1.33 kg in mass). This suggests that the orbits identified in this study could potentially be used to explore Phobos and Deimos as part of a rideshare opportunity, assuming the rideshare could deploy after a stable Mars insertion orbit was achieved by the primary spacecraft. This would allow future Mars missions to significantly expand their science return at a low cost, and at minimal risk to the primary mission.

REFERENCES

[1] Mukhin L. M., Sagdeev R., Karavasili K., and Zakharov A., "Phobos, Deimos Mission," Concepts and Approaches for Mars Exploration, edited by N.G. Barlow, July 200, pp. 230-232.

[2] Sagdeev R. Z. and Zakharov A. V., "Brief History of the PHOBOS Mission," Nature (London), Vol. 341, Oct. 1989, pp. 581-585. do:10.1038/341581a0

[3] Fraeman, A.A., Arvidson, R.E., Murchie, S.L., Rivkin, A., Bibring, J.-P., Choo, T.H., Gondet, B., Humm, D., Kuzmin, R.O., Manaud, N. Zabalueva, E.V., Analysis of disk-resolved OMEGA and CRISM spectral observations of Phobos and Deimos, Journal of Geophysical Research (2015) 117, E00J15, doi:10.1029/2012JE004137, 2012

[4] Fraeman, A.A., Murchie, S.L., Arvidson, R.E., Clark, R.N., Morris, R.V., Rivkin, A.S., Vilas, F., Spectral absorptions on Phobos and Deimos in the visible/near infrared wavelengths and their compositional constraints, Icarus (2014) 229:196-205.

[5] Taylor, J.J. and Faust N.L., Spacecraft Rendezvous with the Martian Moons, Journal of Spacecraft and Rockets, Vol. 10, No. 8 (1973), pp. 520-524.

[6] Tolson, R. H. and Blanchard, R. C. and Daniels, E. F., Phobos and Deimos Encounter Experiment during the Viking Extended Mission, Journal of Spacecraft and Rockets (1976) 13(1), pp. 19-25.

[7] Gill P. J. S. and Schwartz J., "Simulations of Quasi-Satellite Orbits Around Phobos," Journal of Guidance, Control, and Dynamics, Vol. 33, No. 3, May-June 2010, pp. 901-914.

[8] Mark S. Wallace, Jeffrey S. Parker, Nathan J. Strange, and Daniel Grebow, Orbital operations for Phobos and Deimos exploration, AIAA-AAS Astrodynamcis Specialist Conference, Minneapolis, Aug. 13-16 (2012).

*https://gmat.gsfc.nasa.gov/

[9] Zamora M. and Biggs J. D., Natural motion around the Martian moon Phobos: the dynamical substitute of the Libration Point Orbits in an elliptical three-body problem with gravity harmonics, Celest. Mech. Dyn. Astro. (2015) 122:263-302, DOI 10.1007/s10569-015-9619-2.

[10] Genova, A.L., Korsmeyer, D.J., Loucks, M.E., Fan Yang Yang, F.Y., and Lee, P., Trajectory Design for the Phobos and Deimos and Mars Environment Spacecraft, AIAA-AAS Astrodynamcis Specialist Conference, Paper AIAA2016-5681, Long Beach, CA, Sept 13-16, 2016